New Journal of Physics
The open-access journal for physics

Bipolar transport in organic field-effect transistors: organic semiconductor blends versus contact modification

Andreas Opitz[1], **Michael Kraus, Markus Bronner, Julia Wagner and Wolfgang Brütting**

Institute of Physics, University of Augsburg, 86135 Augsburg, Germany
E-mail: Andreas.Opitz@physik.uni-augsburg.de

New Journal of Physics **10** (2008) 065006 (12pp)
Received 31 January 2008
Published 30 June 2008
Online at http://www.njp.org/
doi:10.1088/1367-2630/10/6/065006

Abstract. The achievement of bipolar transport is an important feature of organic semiconductors, both for a fundamental understanding of transport properties and for applications such as complementary electronic devices. We have investigated two routes towards organic field-effect transistors exhibiting bipolar transport characteristics. As a first step, ambipolar field-effect transistors are realized by mixtures of *p*-conducting copper-phthalocyanine (CuPc) and *n*-conducting buckminsterfullerene (C_{60}). As a second step, bipolar transport in copper-phthalocyanine is achieved by a modification of the gate dielectric in combination with a controlled variation of the electrode materials used for carrier injection. The analysis involves the determination of charge-carrier mobilities and contact resistances by a single curve analysis and by the transfer length method. Comparison of both types of samples indicates that percolation is a crucial feature in mixtures of both materials to achieve ambipolar carrier flow, whereas in neat films of one single material suitable contact modification allows for bipolar charge-carrier transport. In the latter case, the obtained electron and hole mobilities differ by less than one order of magnitude.

[1] Author to whom any correspondence should be addressed.

Contents

1. Introduction

The achievement of bipolar transport is an important feature of organic semiconductors (OSCs), both for a fundamental understanding of transport properties and for applications such as complementary electronic devices. Actually, systematic transport studies of organic molecular crystals date back to the 1970s and 80s, when it was demonstrated by time-of-flight measurements that in the bulk of high purity single crystals of several aromatic hydrocarbons there is no fundamental difference between the transport of electrons and holes [1]. Nevertheless, in the subsequently upcoming thin film devices, where charge-carrier transport is strongly affected by contacts and other interfaces, there was the long-standing paradigm of unipolar transport in OSC materials. In particular, organic field-effect transistors (OFETs), where the transport occurs at the interface between an OSC and a dielectric, exhibited in most cases only *p*-type transport. Recently, this paradigm has started to change as people have developed means to improve the injection of both carrier types from the electrodes and to reduce traps at the semiconductor/insulator interface, which can inhibit the transport of one carrier species [2, 3]. Especially, electron traps on silicon dioxide, which is often used as gate insulator in OFETs, were identified as major problems. Using polymer insulators in combination with low-work function calcium electrodes, electron transport has been realized in traditionally *p*-conducting materials, like pentacene or polythiophene [2]–[5]. This suggests that most organic materials are bipolar, implying that both electron and hole transport can be achieved by preventing bulk and interface traps, and by choosing electrodes with an appropriate work function.

Related to the realization of transport of both charge-carrier types is the phenomenon of ambipolar transport. This is the case when both charge-carrier types are being transported in the channel of an OFET at the same time. Ambipolar transport was reported already in the 1970s for hydrogenated amorphous silicon thin film transistors [6]. In the context of OSCs, ambipolar transport was observed in mixtures [7, 8] or double-layers [9, 10] of *p*- and *n*-type materials, with different electrodes for electron and hole injection [11, 12] or by using low-band gap OSCs [7, 13].

In this contribution two material systems will be presented. Firstly, ambipolar transport in mixtures of *p*- and *n*-type semiconductors (fullerene and copper-phthalocyanine) will be investigated by analyzing charge-carrier mobilities and contact resistances as a function of the mixing ratio. Secondly, electron and hole transport will be characterized in neat films of copper-phthalocyanine where modification of the gate dielectric and the choice of suitable contact materials allow for bipolar charge-carrier transport.

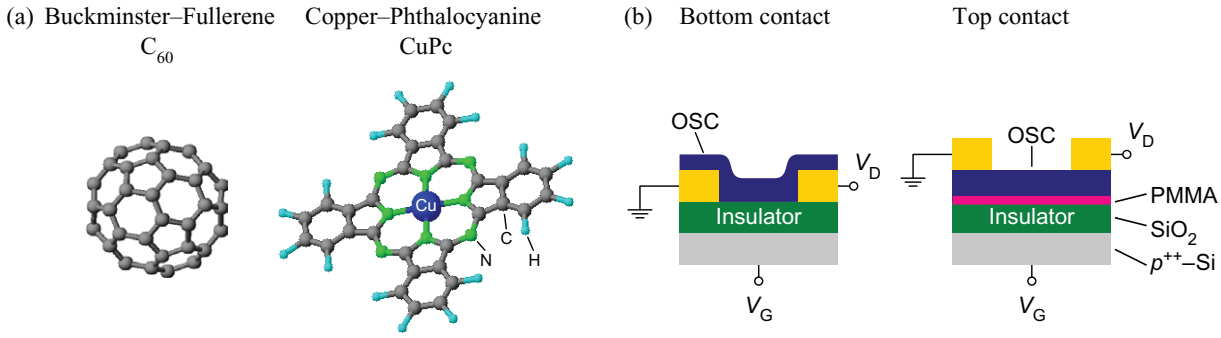

Figure 1. (a) Chemical structures of the used materials: fullerene (C_{60}) and copper-phthalocyanine (CuPc). (b) Side view of bottom contact and top contact structures, both using bottom gate electrodes. (OSC stands for organic semiconductor and PMMA denotes polymethyl methacrylate.)

2. Materials and methods

Copper-phthalocyanine (CuPc, purchased from Sigma Aldrich and additionally purified by temperature gradient sublimation) and buckminsterfullerene (C_{60}, purchased from Sigma Aldrich as sublimation grade) were used as OSCs. The structural formulae are given in figure 1(a). The OSC films were deposited by thermal evaporation from low-temperature effusion cells in a vacuum better than 1×10^{-7} mbar. The thickness of the films was controlled via deposition monitors using quartz microbalances. For mixed films, two independent monitors were used. The deposition rates were 0.35 Å s^{-1} for neat films and up to 1.4 Å s^{-1} for the material with the higher volume fraction in the mixtures. OFETs were fabricated on highly conductive Si wafers (resistivity of 1–5 mΩ cm) with a 320 nm thick thermally grown oxide, which acts as gate insulator (see figure 1(b)).

Samples described in the first part of this contribution incorporate photolithographically patterned Au (100 nm, using 1 nm Ti as adhesion layer) source and drain electrodes made by electron-beam evaporation and a subsequent lift-off process. These structures were cleaned in an ultrasonic bath with solvents (acetone and isopropyl) and ultra-pure water. The substrates were dried with pure nitrogen, treated with an O_2-plasma for 60 s at 200 W and 0.6 mbar, and heated in pre-vacuum at 400 K for 2 h. Transistors with a ring-type geometry were used, whose source electrodes form a closed ring around the drain electrodes. This prevents parasitic currents from the outside of the active transistor channel without the necessity of structuring the OSC [14]. The channel lengths ranged from 5 to 80 μm with a channel width of 2500 μm. Finally, a 25 nm thick film of the organic materials was deposited on top of these prestructured substrates as described above to realize a bottom-gate and bottom-contact OFET.

In the second part of this paper, we show results obtained on bottom-gate and top-contact OFETs. In these devices the SiO_2 surface was first coated by a polymethyl methacrylate (PMMA) film of about 10 nm thickness (measured by surface profilometry) to prevent electron traps [2, 15]. Then a 25 nm thick layer of CuPc was deposited, before the top electrodes were thermally evaporated through a shadow mask to yield interdigitated finger electrodes. In this case, the channel length ranged from 80 to 180 μm with a channel width of 1000 μm. Different metals (Ca, Al, Ag and Au) with a thickness of about 50 nm were used as electrode materials.

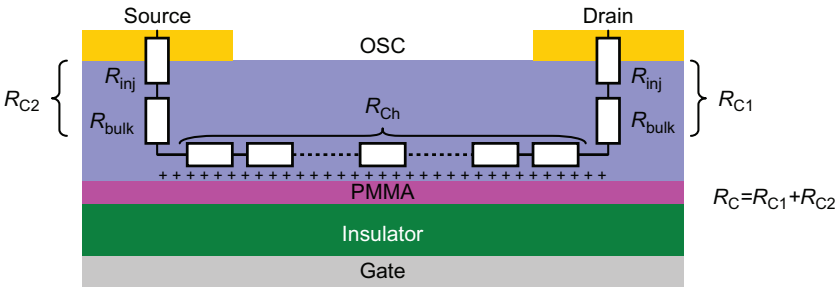

Figure 2. Schematic profile of a transistor channel with the contact resistance R_C (consisting of interface resistances R_{inj} and bulk resistances R_{bulk}) and the channel resistance R_{ch}.

Additionally, fluorinated tetracyanoquinodimethane (F_4TCNQ) ($\approx$1 nm thickness) was used as electron blocking layer between CuPc and a gold or silver electrode.

For characterization the devices were transferred without air-exposure to a vacuum-chamber providing a pressure less than 5×10^{-6} mbar. The output and transfer characteristics of the transistors were measured using a Keithley 4200 Semiconductor Characterisation System.

Two methods are used to determine the mobility and the contact resistance of the OFETs. Following the single curve analysis (SCA) suggested by Horowitz *et al* [16], the drain voltage in the Shockley equation is replaced by the drain voltage corrected for the contact resistance ($V_D \rightarrow V_D - I_D \cdot R_{C,SCA}$). As a result, the drain current is given by

$$I_D = \frac{\mu_{SCA}(W/L)C_{Ins}(V_G - V_T)V_D}{1 + \mu_{SCA}R_{C,SCA}(W/L)C_{Ins}(V_G - V_T)}, \tag{1}$$

where W denotes the field-effect transistor (FET) channel width, L the channel length, C_{Ins} the specific insulator capacitance and μ_{SCA} the mobility. $V_G - V_T$ is the effective gate voltage, where the applied gate voltage V_G is reduced by the threshold voltage V_T, which appears for example due to interface states. Using the channel conductance $g_d = \partial I_D/\partial V_D$ and the transconductance $g_m = \partial I_D/\partial V_G$ the mobility μ_{SCA} and the contact resistance $R_{C,SCA}$ were calculated from

$$\sqrt{\mu_{SCA}}(V_G - V_T) = \frac{g_d}{\sqrt{g_m}}\sqrt{\frac{L V_D}{W C_{Ins}}} \tag{2}$$

and

$$R_{C,SCA} = \frac{1}{g_d} - \frac{1}{\mu_{SCA}(W/L)C_{Ins}(V_G - V_T)}. \tag{3}$$

The second method is called the transfer length method (TLM) [17]. There the total resistance of the OFET is split into contact and channel resistance (see figure 2), with the contact resistance being independent of the channel length. Using the Shockley equation the total resistance can then be described as a constant contact resistance $R_{C,TLM}$ and the channel resistance which is proportional to the channel length for a given channel width:

$$R_{total} = R_{C,TLM} + \frac{L}{\mu_{TLM} W C_{Ins}(V_G - V_T)}. \tag{4}$$

For this analysis the transfer characteristics of OFETs with different channel lengths are measured. A linear fit of the channel resistance versus the channel length yields the contact resistance $R_{C,TLM}$ and the mobility μ_{TLM}.

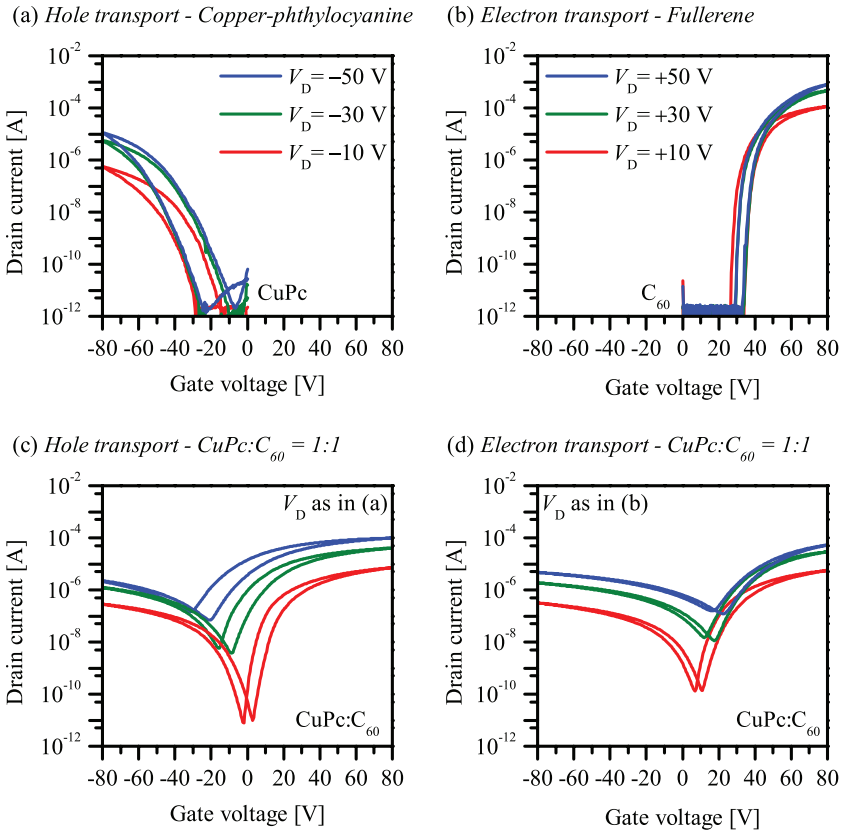

Figure 3. Unipolar OFET transfer characteristics of neat films of CuPc (a) and C_{60} (b) and ambipolar OFET transfer characteristics (c and d) of a 1 : 1 mixture for channel length of 5 μm. (All OFETs shown here are in the bottom-contact configuration.)

It was shown that the charge-carrier mobility of organic materials depends on the charge-carrier density and thereby on the effective gate voltage [18]–[21]. Both mentioned analysis methods are useful to determine the mobility in dependence on the effective gate voltage or the charge-carrier mobility.

3. Ambipolar transport in mixtures of C_{60} and CuPc

In previous works, we have already investigated film morphology, electronic structure and charge-carrier transport in mixtures of C_{60} and CuPc, and have demonstrated possible applications as quasi-complementary inverters [8, 22, 23]. Here, we focus on charge-carrier injection and transport in neat films and blends of these materials. In contrast to previous work, we use materials purified by temperature gradient sublimation and apply two different methods (SCA and TLM) for the extraction of charge-carrier mobility and contact resistance. On the whole, the results are in agreement with previous work, nevertheless, in detail there are some differences, e.g. an increased hole mobility in CuPc is found, which can be traced back to higher material purity.

Figure 3 shows typical transfer characteristics of OFETs with neat CuPc and neat C_{60} in comparison to a 1 : 1 mixture of both materials. For the former two, only unipolar

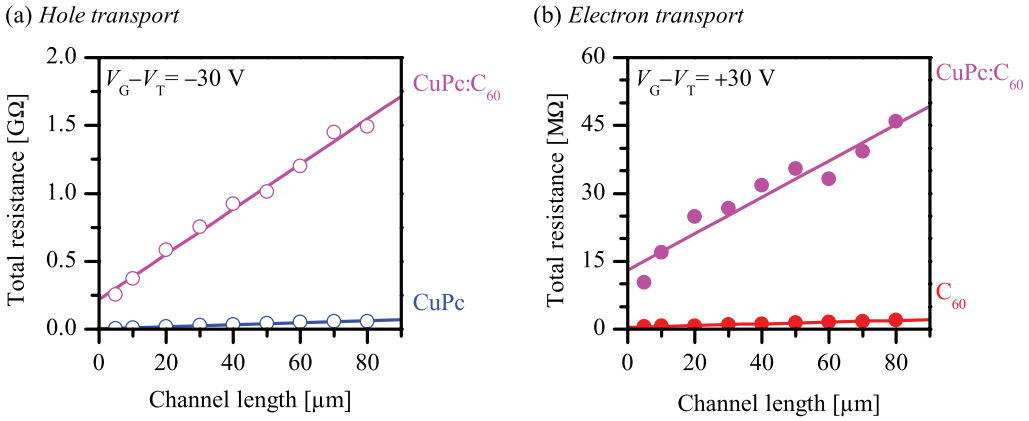

Figure 4. Resistance versus channel length for the TLM applied to OFETs with neat films of C_{60} and CuPc and a 1 : 1 mixture.

transport is observed in the bottom-contact geometry used here. The drain current reaches higher values for the C_{60} FET resulting in a higher mobility. The obtained mobilities are $\mu_h = 1.7 \times 10^{-3}\,cm^2\,V\,s^{-1}$ and $\mu_e = 6.8 \times 10^{-2}\,cm^2\,V\,s^{-1}$ for hole transport in CuPc and electron transport in C_{60}, respectively.

Ambipolar transport is visible by a current increase in the regime where unipolar OFETs are in the off-state. This behaviour appears for mixed films of C_{60} and CuPc both in the *n*- and *p*-channel regimes and is shown in figures 3(c) and (d) for a mixing ratio of 1 : 1. Additionally, a 1 : 3 and a 3 : 1 mixing ratio were investigated and analyzed. The observed ambipolar current increase originates from the injection of the respective minority charge-carrier type at the drain electrode and the transport of them in the channel. As shown in previous publications [8, 11], the charge-carrier mobilities can be consistently determined from both the unipolar and the ambipolar part of the transfer characteristics. The shift of the minimum in the ambipolar transfer curve is related to a shift of the ambipolar region in the transistor channel with the drain voltage and can be described by the model of Schmechel *et al* [11].

Figure 4 shows the analysis of the device resistance for different channel lengths using the TLM. Data are shown for hole transport in CuPc and in a 1 : 1 mixture (figure 4(a)) and for electron transport in C_{60} and a 1 : 1 mixture (figure 4(b)) for an effective gate voltage $|V_G - V_T| = 30$ V. All curves are reasonably well-described by a linear relationship, confirming the applicability of TLM. It is clearly visible that the mixture of C_{60} and CuPc has larger contact resistance (axis intercept) and lower mobility (steeper slope) as compared to the neat films. Furthermore, the contact resistance for holes is larger than for electrons in the mixed film.

Using SCA and TLM analysis the mobilities and the contact resistances were determined for all investigated samples. The dependence of the two quantities on the mixing ratio is summarized in figure 5. The agreement between both analysis methods is remarkable. Whereas the TLM analysis to determine the contact resistance is rather straight-forward, some simplifications are involved in the SCA. In particular, the dependence of the contact resistance on the drain current is neglected and the dependence of the mobility on the gate voltage is not considered in the transconductance (equation (2)). Nevertheless, there is excellent agreement of both the dependence of the mobility and the contact resistance on the mixing ratio.

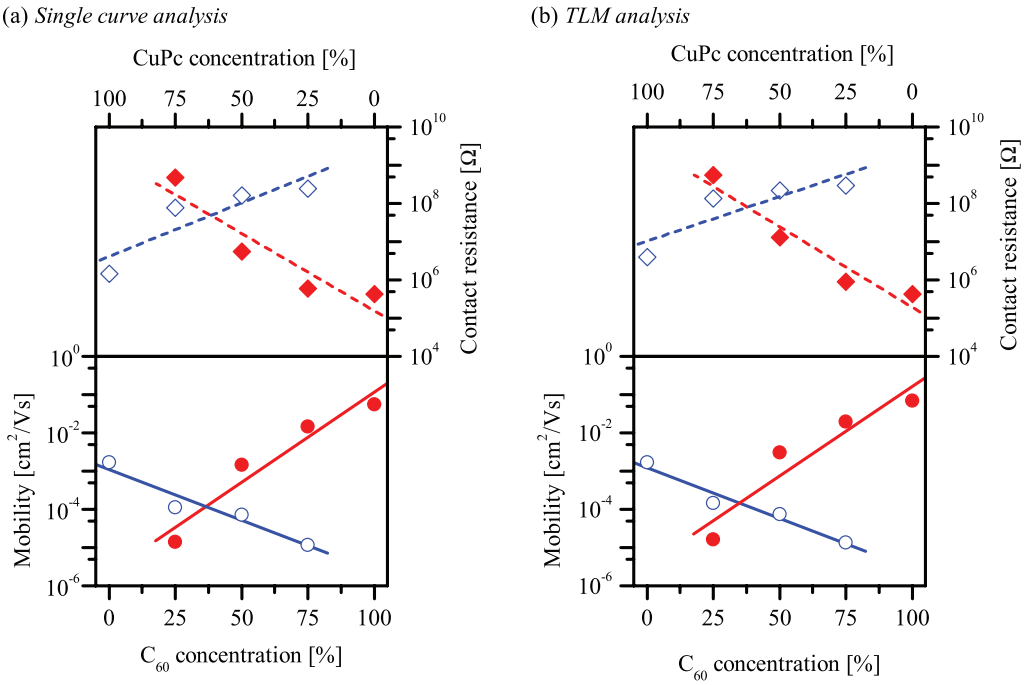

Figure 5. Contact resistance and mobility versus concentration in CuPc:C_{60} mixtures for the SCA (left) and the analysis using TLM (right). The effective gate voltage $|V_G - V_T|$ is 30 V (open symbols: hole transport and filled symbols: electron transport).

In both cases, the mobilities of electrons and holes are found to decrease exponentially with decreasing concentration of the respective transport material. Ambipolar transport occurs for all three investigated mixtures, however, only for a mixture with about 35% C_{60} content would one obtain equal electron and hole mobilities. As reported previously [22]–[25], C_{60} and CuPc are electronically non-interacting so that there is no charge transfer in the ground state. This implies that transport in blends is only possible by separate percolation pathways of electrons and holes in the respective transport material. The decrease of both mobilities upon dilution can then be related to an increased hopping distance between molecules or grains of one material.

In contrast to the mobilities, the contact resistances for electron and hole injection increase with decreasing concentration of the respective transport material. This is at first glance rather unexpected, since the injection barriers as derived from photoelectron spectroscopy are found to decrease upon diluting one material with the other species [22, 23]. However, a plot of the contact resistances obtained on different samples versus the mobilities of the same samples, as shown in figure 6, suggests a correlation between both quantities. In contrast to figure 5, this figure contains data for the whole range of effective gate voltages $|V_G - V_T| = 25$–50 V to include possible effects of the gate voltage dependent mobility, too. In detail, there are some differences between both analysis methods, as the SCA data display quite statistical scatter, whereas the data points from TLM appear in groups with a systematic shift of $R_{C,TLM}$ versus μ_{TLM} with the gate voltage. Taking all data together, however, a reciprocal relation $R_C \sim \mu^{-1}$ is observed for both analysis methods indicating that the low mobility limits the injection of

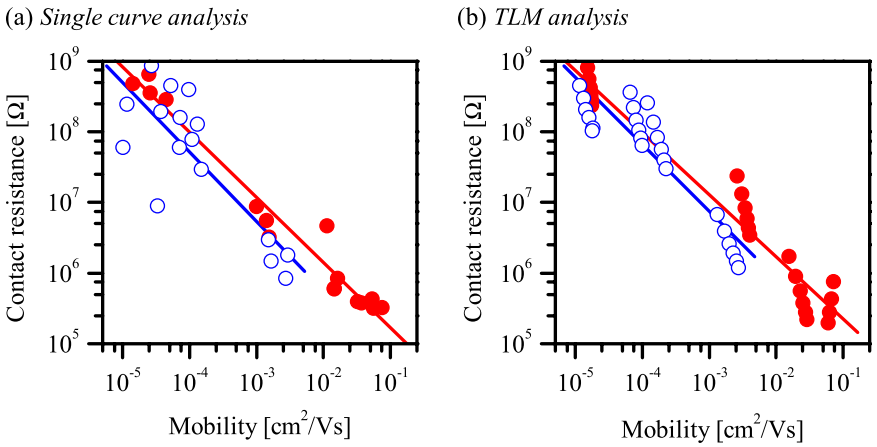

Figure 6. Contact resistance versus mobility for the SCA (left) and the analysis using TLM (right). The effective gate voltage $|V_G - V_T|$ ranges from 25 to 50 V (open symbols: hole transport and filled symbols: electron transport).

charge carriers. This behaviour can be explained by diffusion limited injection [26] following the equation

$$j_{inj} \sim \mu \exp\left[-\frac{\Phi_B}{kT}\right], \tag{5}$$

where Φ_B denotes the injection barrier, which also shows some variation [22], but due to the large changes of the mobility with the composition of the blend is not the dominant factor. Similar behaviour was observed in hole-only diodes [27], where the mobility was varied by mixing semiconducting and insulating molecules, as well as in unipolar OFETs [28], where the mobility was changed by the charge-carrier concentration.

4. Electron and hole transport in neat films of CuPc

In the preceding section, we presented measurements on ambipolar OFETs consisting of blends of CuPc and C_{60} deposited on Si–SiO_2 substrates. However, there is also the possibility to achieve transport of both carrier types (holes as well as electrons) in a neat layer of CuPc, which will be the topic in this section.

As was shown with pentacene, polythiophene and other hole conductors, a prerequisite for achieving electron transport in such classical *p*-type materials is a suitable passivation of electron traps at the surface of the SiO_2 gate dielectric, e.g. by a non-polar polymer interlayer [2, 5, 15]. Additionally, it is necessary to chose low-work function metals to allow for sufficiently high electron injection into the OSC [2, 3]. Thus, for our investigations we have coated the SiO_2 substrates with a thin layer of PMMA and have used top contacts patterned by evaporation through a shadow mask. Figure 7 shows transfer characteristics for three different source and drain electrode materials. OFETs with gold contacts exhibit ambipolar transport, while those with F_4TCNQ/gold exclusively show hole transport and others with calcium exclusively show electron transport. Additionally, silver, F_4TCNQ/silver and aluminium were used as electrode materials (not shown). They were found to exhibit the same behaviour as gold, F_4TCNQ/gold and calcium, respectively.

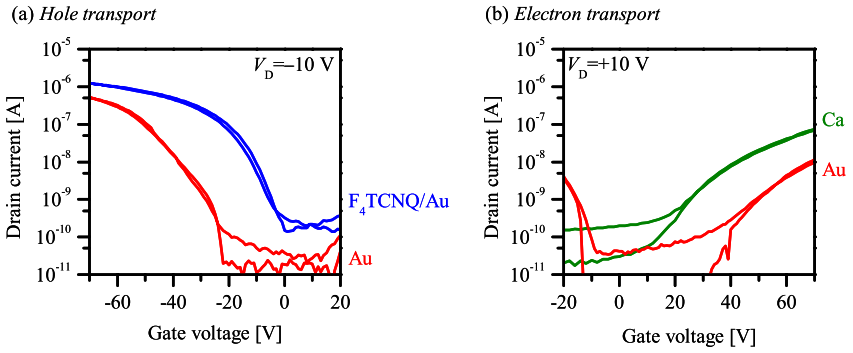

Figure 7. Transfer characteristics of CuPc FETs in the top-contact configuration with different electrodes: calcium, gold and F_4TCNQ/gold.

Table 1. Collection of the mobilities determined in top-contact OFETs by the SCA and the TLM for various electrodes together with the work functions obtained by Kelvin probe and the contact resistances determined by SCA (n.d., not determined). For comparison, the ionization potential and the electron affinity of CuPc are at 5.0 and 2.7 eV [22, 24], respectively.

	SCA		TLM		SCA		
Electrode material	Electron mobility ($cm^2\,V\,s^{-1}$)	Hole mobility ($cm^2\,V\,s^{-1}$)	Electron mobility ($cm^2\,V\,s^{-1}$)	Hole mobility ($cm^2\,V\,s^{-1}$)	*n*-channel contact resistance (Ω)	*p*-channel contact resistance (Ω)	Work function (eV)
Calcium	1.4×10^{-4}	–	2.5×10^{-4}	–	1.7×10^{8}	–	3.3
Aluminium	n.d.	–	4.4×10^{-4}	–	n.d.	–	3.6
Silver	1.1×10^{-4}	2.0×10^{-3}	5.4×10^{-4}	1.4×10^{-3}	4.5×10^{8}	3.4×10^{7}	4.9
Gold	8.6×10^{-5}	1.9×10^{-3}	1.4×10^{-4}	1.7×10^{-3}	4.4×10^{8}	2.5×10^{7}	5.0
F_4TCNQ/Silver	–	2.4×10^{-3}	–	1.8×10^{-3}	–	2.3×10^{7}	5.3
F_4TCNQ/Gold	–	1.8×10^{-3}	–	2.5×10^{-3}	–	1.3×10^{7}	5.6

The field-effect mobilities of all devices were determined by SCA and TLM analysis and are listed in table 1. There is a clear asymmetry in hole and electron mobility, with the hole mobility being about one order of magnitude higher. The average values of the field-effect mobility are $\mu_e = 3.4 \times 10^{-4}\,cm^2\,V\,s^{-1}$ for electrons and $\mu_h = 1.8 \times 10^{-3}\,cm^2\,V\,s^{-1}$ for holes. The same asymmetry and comparable absolute numbers have already been observed for CuPc single crystals [29]. Important to note, when the contact resistance is accounted for, the hole mobility of CuPc is the same in bottom- and top-contact FETs (see the previous section). It can also be seen that the choice of the electrode material has no significant effect on the mobility of each carrier type. Thus, the field-effect mobilities determined here can be considered as an intrinsic property of CuPc thin films.

Comparing the sample with gold contacts to the one with F_4TCNQ/gold contacts, a strong decrease of the threshold voltage $|V_T|$ is remarkable while the change of the mobility is only marginal. It has already been demonstrated for pentacene that a thin layer of F_4TCNQ on top of the OSC can control the threshold gate voltage but has no effect on the field-effect mobility

and the on/off ratio of the transistor [30]. This is in good agreement with our results for CuPc. Furthermore, we have obtained comparable results when silver and F_4TCNQ/silver electrodes were used.

The contact resistances as determined by the SCA method are listed in table 1. (Note that the TLM does not provide very reliable values for the contact resistance in our top-contact OFETs, because with evaporated finger electrodes the channel length could not be determined as precisely as with photolithographically patterned source–drain electrodes.) The contact resistance for electron transport is about one order of magnitude higher than that for hole transport. This is again correlated to the higher mobility of holes and is an indication for diffusion-limited transport. In detail, it is not straightforward to compare the contact resistances for various electrode materials since the materials differ with respect to their chemical properties and diffusive behaviour. Evaporated gold, e.g., tends to diffuse into the organic layer whereas other materials remain on top of it [31]. This diffusion can reduce the contact resistance but has no effect on the channel resistance.

The work functions of the electrode materials were determined by Kelvin probe measurements (see table 1). It has to be mentioned that the accessible electrode surface in the Kelvin probe measurements does not necessarily have the same effective work function as the evaporated contact on top of the CuPc layer. Thus, the given work functions should only be taken as approximate values.

Calcium and aluminium have the lowest work function. Consequently, they only act as electron injectors. The work function of silver and gold is about 1.5 eV higher. These materials are therefore suitable for both electron and hole injection into the CuPc layer which is actually observed as ambipolar transport. The question why F_4TCNQ/gold exclusively reveals hole injection, although its work function is only slightly higher than that for gold, may be explained by the tendency of F_4TCNQ to block electron injection [32], while the injection of holes is also improved. This assumption is confirmed by the fact that the contact resistance for holes is smallest with F_4TCNQ/gold as injecting contact.

5. Summary

We have investigated two routes towards bipolar transport in organic FETs. Firstly, using mixtures of different *p*- and *n*-type organic materials and secondly by adjusting the electrode work function for electron and hole injection into a single material. Although both routes are in principle successful, there are some characteristic differences.

Mixtures of CuPc und C_{60} exhibit a strong dependence of the electron and hole mobilities on the mixing ratio, which indicates that percolation is the limiting parameter. Thus, achieving (am)bipolar transport inevitably involves a dilution of the respective transport material by the other species and thus a strong reduction of the mobilities for both carrier types as compared to the neat systems. Additionally, as the injection process is found to be diffusion limited, these blends exhibit increased contact resistances. Nevertheless, such ambipolar mixtures are frequently used in so-called bulk-heterojunction photovoltaic cells. Thus, the presented results are expected to have implications not only for OFETs but also for other organic electronic devices.

In the second part of this work, we have demonstrated that neat films of a single OSC, in this case CuPc, can exhibit both electron and hole transport as well as ambipolar transport, if the surface of the gate dielectric is passivated in order not to trap electrons and if contacts with

suitable work function are used. In this case, the electron and hole mobilities are independent of the electrode material so that intrinsic mobility data are accessible. For the investigated CuPc there is an asymmetry between the electron and hole mobility, however, the difference is only a factor of 10.

Acknowledgments

This work was supported by the Deutsche Forschungsgemeinschaft through Schwerpunktprogramm 1121 and Sonderforschungsbereich 484. We thank Jens Pflaum (University of Stuttgart) for purifying organic materials.

References

[1] Karl N 1985 *Organic Semiconductors* (*Landolt-Boernstein* (*New Series*)*, Group III* vol 17 *Semiconductors*) ed O Madelung, M Schulz and H Weiss (Berlin: Springer) pp 106–218 (Updated edition: vol 41E 2000)

[2] Chua L L, Zaumseil J, Chang J F, Ou E C W, Ho P K H, Sirringhaus H and Friend R H 2005 General observation of *n*-type field-effect behaviour in organic semiconductors *Nature* **434** 194–9

[3] Yasuda T, Goto T, Fujita K and Tsutsui T 2004 Ambipolar pentacene field–effect transistors with calcium source–drain electrodes *Appl. Phys. Lett.* **85** 2098–100

[4] Ahles M, Schmechel R and von Seggern H 2004 *N*-type organic field-effect transistor based on interface-doped pentacene *Appl. Phys. Lett.* **85** 4499–501

[5] Ahles M, Schmechel R and von Seggern H 2005 Complementary inverter based on interface doped pentacene *Appl. Phys. Lett.* **87** 113505

[6] Neudeck G W and Malhotra Mis A K 1975 Field-effect conductance modulation in vacuum-evaporated amorphous silicon films *J. Appl. Phys.* **46** 239–47

[7] Meijer E J, De Leeuw D M, Setayesh S, Van Veenendaal E, Huisman B H, Blom P W M, Hummelen J C, Scherf U and Klapwijk T M 2003 Solution-processed ambipolar organic field-effect transistors and inverters *Nat. Mater.* **2** 678–82

[8] Opitz A, Bronner M and Brütting W 2007 Ambipolar charge carrier transport in mixed organic layers of phthalocyanine and fullerene *J. Appl. Phys.* **101** 063709

[9] Rost C, Gundlach D J, Karg S and Rieß W 2004 Ambipolar organic field-effect transistor based on an organic heterostructure *J. Appl. Phys.* **95** 5782–7

[10] Wang J, Wang H B, Yan X J, Huang H C and Yan D H 2005 Organic heterojunction and its application for double channel field-effect transistors *Appl. Phys. Lett.* **87** 093507

[11] Schmechel R, Ahles M and von Seggern H 2005 A pentacene ambipolar transistor: experiment and theory *J. Appl. Phys.* **98** 084511

[12] Swensen J S, Yuen J, Gargas D, Buratto S K and Heeger A J 2007 Light emission from an ambipolar semiconducting polymer field effect transistor: analysis of the device physics *J. Appl. Phys.* **102** 013103

[13] Smits E C P, Anthopoulos T D, Setayesh S, van Veenendaal E, Coehoorn R, Blom P W M, de Boer B and de Leeuw D M 2006 Ambipolar charge transport in organic field-effect transistors *Phys. Rev.* B **73** 205316

[14] Meijer E J, Detcheverry C, Baesjou P J, van Veenendaal E, de Leeuw D M and Klapwijk T M 2003 Dopant density in disordered organic field-effect transistors *J. Appl. Phys.* **93** 4831–5

[15] Benson N, Melzer C, Schmechel R and von Seggern H 2008 Electronic states at the dielectric/semiconductor interface in organic field effect transistors *Phys. Status Solidi* a **205** 475–87

[16] Horowitz G, Hajlaoui R, Fichou D and El Kassmi A 1999 Gate voltage dependent mobility of oligothiophene field-effect transistors *J. Appl. Phys.* **85** 3202–6

[17] Klauk H, Schmid G, Radlik W, Weber W, Zhou L, Sheraw C D, Nichols J A and Jackson T N 2003 Contact resistance in organic thin film transistors *Solid-State Electron.* **47** 297–301

[18] Schauer F 1999 Temperature dependent field effect in organic-based thin-film transistor and its spectroscopic character *J. Appl. Phys.* **86** 524–31
[19] Tanase C, Blom P W M, de Leeuw D M and Meijer E J 2004 Charge carrier density dependence of the hole mobility in poly(p-phenylene vinylene) *Phys. Status Solidi* a **201** 1236–45
[20] Butko V Y, Lashley J C and Ramirez A P 2005 Low-temperature field effect in a crystalline organic material *Phys. Rev. B* **72** 081312
[21] Salleo A 2007 Charge transport in polymeric transistors *Mater. Today* **10** 38–45
[22] Opitz A, Bronner M, Brütting W, Himmerlich M, Schaefer J A and Krischok S 2007 Electronic properties of organic semiconductor blends: ambipolar mixtures of phthalocyanine and fullerene *Appl. Phys. Lett.* **90** 212112
[23] Bronner M, Opitz A and Brütting W 2008 Ambipolar charge carrier transport in organic semiconductor blends of phthalocyanine and fullerene *Phys. Status Solidi* a **205** 549–63
[24] Molodtsova O V and Knupfer M 2006 Electronic properties of the organic semiconductor interfaces CuPc/C_{60} and C_{60}/CuPc *J. Appl. Phys.* **99** 053704
[25] Lozzi L, Granato V, Picozzi S, Simeoni M, La Rosa S, Delly B and Santucci S 2006 CuPc : C_{60} blend film: a photoemission investigation *J. Vac. Sci. Technol.* A **24** 1668–75
[26] Sze S 1982 *Physics of Semiconductor Devices* (New York: Wiley)
[27] Shen Y L, Klein M W, Jacobs D B, Scott J C and Malliaras G G 2001 Mobility-dependent charge injection into an organic semiconductor *Phys. Rev. Lett.* **86** 3867–70
[28] Hamadani B H and Natelson D 2004 Temperature-dependent contact resistances in high-quality polymer field-effect transistors *Appl. Phys. Lett.* **84** 443–5
[29] de Boer R W I, Stassen A F, Craciun M F, Mulder C L, Molinari A, Rogge S and Morpurgo A F 2005 Ambipolar Cu- and Fe-phthalocyanine single-crystal field-effect transistors *Appl. Phys. Lett.* **86** 262109
[30] Abe Y, Hasegawa T, Takahashi Y, Yamada T and Tokura Y 2005 Control of threshold voltage in pentacene thin-film transistors using carrier doping at the charge-transfer interface with organic acceptors *Appl. Phys. Lett.* **87** 153506
[31] Koch N 2007 Organic electronic devices and their functional interfaces *ChemPhysChem* **8** 1438–55
[32] Minari T, Miyadera T, Tsukagoshi K, Aoyagi Y and Ito H 2007 Charge injection process in organic field-effect transistors *Appl. Phys. Lett.* **91** 053508